Supplementary Online Content

Sheean RK, McKay FC, Cretney E, et al. Association of regulatory T-cell expansion with progression of amyotropic lateral sclerosis: a study of humans and a transgenic mouse model. *JAMA Neurol*. Published online March 5, 2018. doi:10.1001/jamaneurol.2018.0035

This supplementary material has been provided by the authors to give readers additional information about their work.

eMethods. Supplementary Methods

Flow cytometry for animal experiments

Peripheral blood (200 µl) was collected from $SOD1^{G93A}$ mice (n = 5 per group) and age-matched WT controls (n = 4 per group) at P100. Blood was collected in EDTA-coated and lymphocytes and mononuclear cells isolated by passing cells through a histopaque-1077 (Sigma-Aldrich, MO, USA) gradient. Cells were stained with mouse surface marker-specific mAbs (from eBioscience CA, USA, unless stated otherwise) including: anti-GITR-allophycocyanin (APC) (DTA-1), anti-CD25-phycoerythrin (PE) (PC61.5), anti-ICOS-PECy7 (7E.17G9), anti-CD8-Alexa Fluor 680 (A680) (53.6.7) (produced at The Walter and Eliza Hall Institute of Medical Research (WEHI), VIC, Australia), anti-CD4-fluoroscein isothiocyanate (FITC) (GK1.5) (produced at WEHI), anti-CD62L-V450 (MEL-14) (BD Biosciences, CA, USA). Intracellular staining was performed using the Foxp3 staining kit (eBioscience) according to the manufacturer's protocol. The Foxp3 staining kit was used for staining of Foxp3 (anti-Foxp3-APC or –Pacific Blue (FJK-16s)) and CTLA4 (anti-CTLA4-PE (UC10-4B9) all from eBioscience. Viable cells were identified by fixable viability dye eFluor 506 (eBioscience) exclusion. Flow cytometry analysis was performed on a FACSCanto II (BD Biosciences) and data processed using FlowJo (Tree Star Incorporated, OR, USA) software.

Quantitative reverse transcription polymerase chain reaction

Lumbar spinal cords (P90) and sciatic nerves (P75) from mice (n=5 mice per group) were rapidly dissected and flash frozen in liquid nitrogen. Total RNA was isolated using the RNeasy Lipid Tissue Mini Kit (Qiagen) and 1000 ng of RNA reverse transcribed into cDNA using the SuperScript® VILO cDNA Synthesis Kit (Invitrogen) according to the manufacturer's recommendations. Real-time PCR was carried out on 20 ng of cDNA using the SsoAdvanced Universal SYBR GRN Master Mix (Bio-Rad) on a CFX96 Touch System (Bio-Rad) using primers against *Foxp3*: forward 5'- CCCATCCCCAGGAGTCTTG-3' and reverse 5'-ACCATGACTAGGGGCACTGTA-3'; *Gata3*: forward 5'- CTCGGCCATTCGTACATGGAA-3' and reverse 5'-GGATACCTCTGCACCGTAGC-3'; *Gdnf*: forward 5'- ATGGGATTCGGGCCACTTG-3' and reverse 5'-ACAGCCACGACATCCCATAA-3'; *Retnla*: forward 5'- TATGAACAGATGGGCCTCCT-3' and reverse 5'-CGAGTAAGCACAGGCAGTTG-3' and mRNA levels were normalised to *Hprt1*: forward 5'-GATCAGTCAACGGGGGACAT-3' and reverse 5'-CATTTTGGGGCTGTACTGCTT-3'. Primers were designed using PrimerBank and synthesised by Geneworks. Data was analysed using the ΔΔCT method [1] using the reference gene *Hprt1* and expressed relative to WT mice.

Behavioural analysis

Body weight and locomotor function of mice were analysed weekly from P60 using an accelerating Mouse Rota-Rod 47600 (Ugo Basile, Monvalle, Italy). At P60, vehicle (n = 9) and IL-2c (n=10) mice were trained on the rotarod by performing a 5 min session at a constant speed (20 rpm), followed by two 5 min session at accelerating speed (4-40 rpm) with 10 min rest periods between each training session. The following day, mice were tested twice at 4-40 rpm (5 min) and the average latency to fall recorded. Age of disease onset and onset of motor dysfunction were determined using the age of peak body weight and rotarod performance, respectively, as previously described [2]. For survival analysis, mice were killed by lethal injection at disease endstage which was objectively determined by the onset of hindlimb paralysis.

Histology and immunohistochemistry

Mice were transcardially perfused using PBS and then cold 4% paraformaldehyde (PFA) in 0.1M phosphate buffer. Lumbar spinal cords (n=5 mice per group) were dissected out, post-fixed overnight at 4° C, then washed twice in PBS and stored in 30% (w/v) sucrose in PBS at 4° C. Cords were embedded in OCT, frozen in isopentane-cooled in liquid nitrogen and later serially cut in horizontal sections (20 µm) for histology and immunohistochemistry. For histology, sections were stained with a 0.5% (w/v) cresyl violet standard protocol, dehydrated and coverslipped using DePex mounting medium (VWR, Australia). Motor neurons were identified according to their morphology, size (>20 µm diameter), ventral horn location and distinct nucleolar profile. For determination of motor neuron areas, 10 cross sections of spinal cord were analysed per animal. Motor neuron size (μm^2) was determined automatically with ImageJ version 1.47v software (Rasband, W.S., ImageJ, U. S. National Institutes of Health, Bethesda, Maryland, USA, http://imagej.nih.gov/ij/, 1997-2016).

For immunohistochemistry, lumbar spinal cord sections were permeabilised with 0.4% (v/v) Triton X-100 for 10 min, blocked in 5% skim milk in PBS and incubated with rabbit NeuN (1:500, ab104225, Abcam), mouse glial fibrillary acidic protein (GFAP) (1:200, MAB360, Millipore), mouse CD11b/OX42 (1:100, MCA275GA, Serotec) or rabbit CD3 (1:500, Dako) primary antibodies overnight at 4° C. The following day sections were incubated in Alexa Fluor-conjugated secondary antibodies (1:200, Molecular Probes, Life Technologies, Mulgrave, Victoria, Australia) for 2 h at room temperature, incubated with Hoechst 33342 (1:10,000) for 15 min and coverslipped using fluorescent mounting medium (Dako, North Sydney, NSW, Australia). Sections were imaged using a Zeiss Axio Observer Z1 inverted research microscope (Carl Zeiss Pty. Ltd, North Ryde, New

South Wales, Australia). For quantification, at least 3 cross sections of spinal cord per mouse were captured with identical exposure settings and quantitative image analysis performed using ImageJ software. Images were converted to 8-bit grayscale and integrated density measurements of ventral horns were determined for each marker, averages was taken and expressed as a percentage of vehicle mice.

REFERENCES

1. Pfaffl MW. A new mathematical model for relative quantification in real-time RT-PCR. Nucleic Acids Res 2001;29:e45.
2. Turner BJ, Parkinson NJ, Davies KE, Talbot K. Survival motor neuron deficiency enhances progression in an amyotrophic lateral sclerosis mouse model. Neurobiol Dis 2009;34:511-517.

Supplementary Table 1. Immune cell subsets in ALS and healthy controls.

Subset	Absolute count**			As % Leukocytes			As % CD4		
	Healthy controls	**ALS**	**p value**	**Healthy controls**	**ALS**	**p value**	**Healthy controls**	**ALS**	**p value**
White blood cells (Leukocytes)	6.0 (3.9 - 10.5)	6.0 (3.6 - 8.5)	0.724	100	100	>0.999			
Neutrophils	3.6 (1.8 - 6.3)	3.8 (1.8 - 6.1)	0.596	60 (37 - 73)	64 (38 - 81)	0.107			
Lymphocytes	***1.8 (1.1 - 3.2)***	***1.5 (0.7 - 3.0)***	***0.035†***	30 (17-49)	26 (11-48)	0.074			
Monocytes	0.4 (0.2 - 0.7)	0.4 (0.2 - 0.6)	0.922	6 (4-10)	6 (4-14)	0.974			
Eosinophils	0.2 (0.0 - 0.8)	0.1 (0.0 - 0.4)	0.173	3 (0-14)	2 (0 - 8)	0.378			
Basophils	0.0 (0.0 - 0.1)	0.0 (0.0 - 0.1)	0.423	0 (0-2)	0 (0-2)	0.511			
$CD4^+$ lymphocytes:	***600 (220-1530)***	***480 (210-1390)***	***0.035†***	10 (4-19)	8 (3-20)	0.053			
$CD4^+CD45RA^+$	220 (50-650)	220 (80-500)	0.834	3.6 (0.8 - 8.7)	3.8 (0.9 -10.0)	0.923	***37 (11-62)***	***41 (17-75)***	***0.042†***
$CD4^+CD45RO^+$	***380 (150-1190)***	***290 (80-890)***	***0.007†***	***6.6 (3.2 - 14.4)***	***5.4 (1.3 -12.6)***	***0.017†***	***63 (38-89)***	***59 (25-83)***	***0.045†***
Treg ($CD4^+CD25^{hi}$ $CD127^{lo}$)	37 (9-99)	33 (19-97)	0.233	0.64 (0.2-1.7)	0.56 (0.3-1.7)	0.274	6.6 (3-12)	6.8 (4-12)	0.325
$CD45RA^+$Treg	8.0 (2-20)	7.3 (3-25)	0.670	0.13 (0.04-0.37)	0.13 (0.04-0.55)	0.884	1.3 (0.4-5.2)	1.6 (0.7-4.3)	0.182
$CD45RO^+$Treg	29 (7-86)	23 (13-75)	0.142	0.42 (0.1-1.4)	0.46 (0.2-1.3)	0.163	5.1 (2.6-8.8)	5.1 (2.2-11.4)	0.848
$FoxP3^+$Treg ($CD4^+CD25^{hi}$ $CD127^{lo}FoxP3^+$)	30 (5-85)	27 (15-92)	0.434	0.52 (0.1-1.5)	0.46 (0.2-1.6)	0.461	5.4 (2-9)	5.7 (3-11)	0.222
$CD45RA^+$Treg $FoxP3^+$	4.5 (0.5-17)	5 (1.7-23)	0.458	0.079 (0.01-0.28)	0.088 (0.03-0.35)	0.468	***0.81 (0.2-3.5)***	***1.12 (0.4-3.9)***	***0.035†***
$CD45RO^+$Treg $FoxP3^+$	24 (5-77)	21 (12-72)	0.209	0.39 (0.1-1.3)	0.37 (0.2-1.3)	0.245	4.4 (2-8)	4.4 (2-11)	0.628
$CD45RA^+$TregCD31$^+$ ($CD4^+CD45RA^+$ $CD25^{hi}$	1.73 (0.25-7.5)	1.46 (0.3-8.6)	0.423	0.42 (0.2-1.5) x 10^{-3}	0.41(0.03-1.6) x 10^{-3}	0.690	2.6 (0.6-20)x 10^{-3}	3.1 (0.6-17)x 10^{-3}	0.843

$CD127^{lo}CD31^{+}$)									

*ALS: n = 33, CON: n = 38; Median and ranges given

** (x 10^9/L) Determined by full blood count (FBC); or (x 10^6/L) for $CD4^{+}$ and $CD4^{+}$subsets, by dual platform analysis using absolute lymphocyte counts from FBC with proportion of total lymphocytes from flow cytometry.

p values calculated by Mann-Whitney test without correction for multiple comparison; †significant p values and corresponding data in bold italic

Supplementary Table 2. Correlation of disease progression rate with frequencies of CD4 T cell subsets expressed as proportions or absolute counts.

CD4 Subset	Correlation[1] of disease progression rate with frequency of CD4 subsets			
	As percentage of leukocytes		Absolute counts (x 10^6/L)	
	r	**p**	***r***	**p**
CD4	***-0.358***[2]	***0.041***[2]	***-0.356***	***0.042***
$CD4^+CD45RA^+$	-0.306	0.083	-0.344[2]	0.050[2]
$CD4^+CD45RO^+$	-0.316[2]	0.073[2]	-0.327	0.063
Total Tregs ($CD4^+CD25^{hi}CD127^{lo}$)	***-0.395***	***0.023***	***-0.401***	***0.021***
$CD45RO^+$Tregs	***-0.371***	***0.034***	***-0.376***	***0.031***
$CD45RA^+$Tregs	-0.190	0.289	-0.202	0.260
$CD45RA^+CD31^+$Tregs	-0.100	0.581	-0.100	0.581
Total $FoxP3^+$Tregs	***-0.411***	***0.018***	***-0.400***	***0.021***
$CD45RO^+$ $FoxP3^+$Tregs	***-0.394***	***0.023***	***-0.378***	***0.030***
$CD45RA^+$ $FoxP3^+$Tregs	-0.202	0.261	-0.206	0.251
$CD45RA^+FoxP3^+$ $CD31^+$Tregs	-0.094	0.603	-0.094	0.604

[1]Pearson's correlation of disease progression with transformed (LN) data is presented; except where raw data fit assumptions of Pearson's correlation and was used as indicated[2].

Supplementary Table 3. Correlation of age with frequencies of CD4 T cell subsets expressed as proportions or absolute counts.

CD4 Subset	Correlation* of age with frequency of CD4 subsets							
	Healthy controls				**ALS**			
	As percentage of leukocytes		Absolute counts (x 10^6/L)		As percentage of leukocytes		Absolute counts (x 10^6/L)	
	r	**p**	***r***	**p**	***r***	**p**	***r***	**p**
CD4	0.066[2]	0.692[2]	0.086	0.607	-0.142	0.430	-0.218	0.224
$CD4^+CD45RA^+$	0.063[2]	0.707[2]	-0.006	0.971	-0.153	0.396	-0.134[2]	0.457[2]
$CD4^+CD45RO^+$	0.041[2]	0.805[2]	0.081	0.627	-0.141	0.433	-0.205	0.251
Total Tregs ($CD4^+CD25^{hi}$ $CD127^{lo}$)	0.092	0.583	0.082[2]	0.624[2]	0.994	0.758	-0.122	0.501
$CD45RO^+$Tregs	0.166	0.320	0.174	0.297	0.060	0.739	0.001	0.994
$CD45RA^+$Tregs	-0.187[2]	0.260[2]	-0.163[2]	0.327[2]	***-0.395***	***0.023***	***-0.464***	***0.007***
$CD45RA^+CD31^+$ Tregs	-0.314	0.055	-0.317	0.053	***-0.487***	***0.004***	***-0.525***	***0.002***
Total $FoxP3^+$Tregs	0.108	0.520	0.126	0.451	-0.035	0.844	-0.099	0.585
$CD45RO^+$ $FoxP3^+$ Tregs	0.185	0.266	0.195	0.241	0.080	0.657	0.017	0.924
$CD45RA^+$ $FoxP3^+$ Tregs	-0.277[2]	0.093[2]	-0.250[2]	0.130[2]	***-0.411***	***0.018***	***-0.455***	***0.008***
$CD45RA^+FoxP3^+$ $CD31^+$ Tregs	-0.294	0.074	-0.276	0.093	***-0.518***	***0.002***	***-0.537***	***0.001***

[1]Pearson's correlation of disease progression with transformed (LN) data is presented; except where raw data fit assumptions of Pearson's correlation and was used as indicated[2].

Supplementary Figure 1

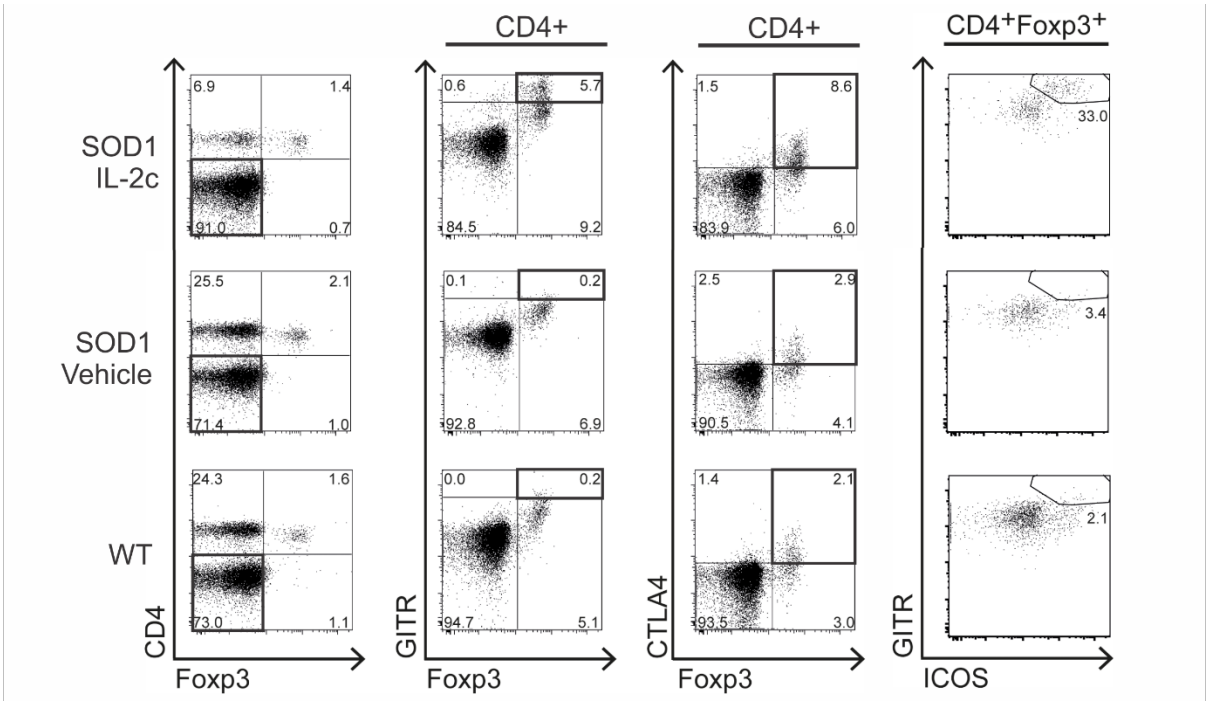

Supplementary Figure 1. Regulatory T cell (Treg) subsets in WT and SOD1^{G93A} mice. Representative flow cytometric analysis of Treg cell populations in peripheral blood isolated from WT, vehicle and IL-2c treated SOD1^{G93A} mice at 100 days of age. Numbers in quadrants and 'gate' represent the percentage of cells in each. FoxP3^{+} Tregs, GITR^{hi} Tregs, CTLA4^{+} Tregs and ICOS^{hi}GITR^{hi} Tregs are highlighted.

Supplementary Figure 2

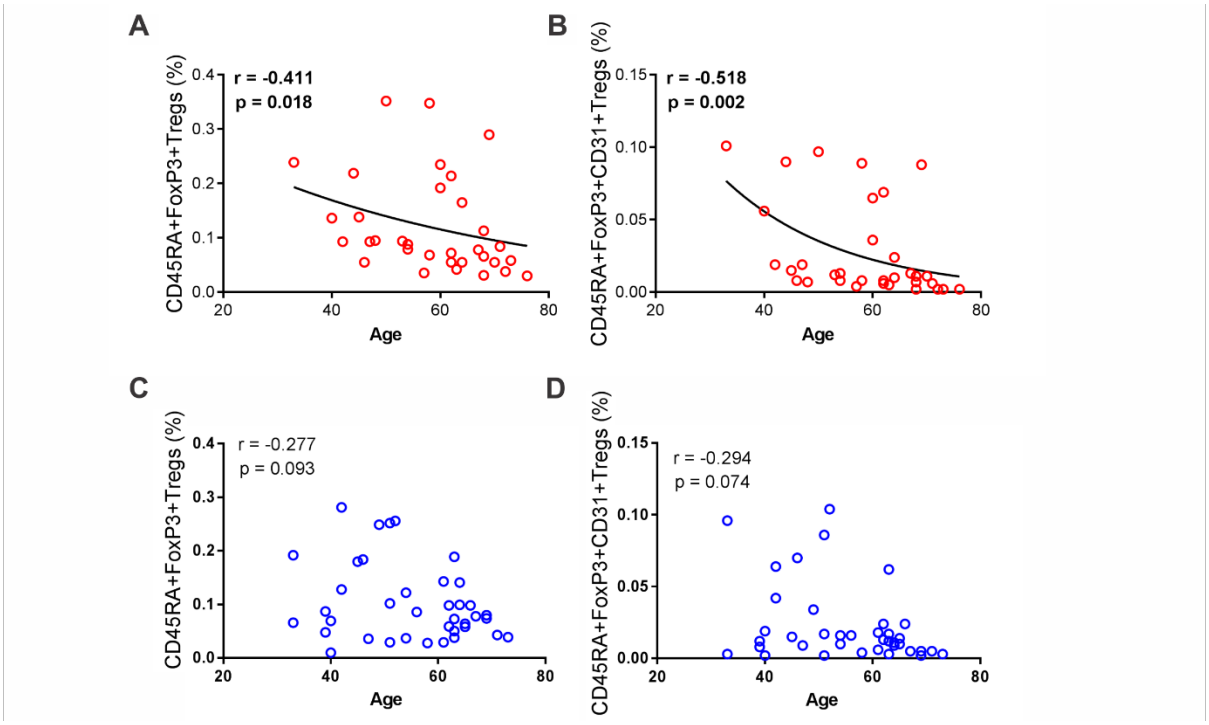

Supplementary Figure 2. Resting peripheral blood regulatory T cells (Tregs) are inversely correlated with age in ALS patients.

Correlation of age with **(A)** $CD45RA^{+}FoxP3^{+}$ Treg and **(B)** $CD45RA^{+}FoxP3^{+}CD31^{+}$ Treg subsets determined as a percentage of leukocytes in ALS patients (n = 33) is shown. There is no correlation of age with **(C)** $CD45RA^{+}FoxP3^{+}$ Treg and **(D)** $CD45RA^{+}FoxP3^{+}CD31^{+}$ Treg subsets in healthy controls (n = 38). Frequencies were determined as a percentage of all leukocytes and Pearson's correlation was used for all (on $\log_e$-transformed cell subsets frequency for A,B,D).

Supplementary Figure 3

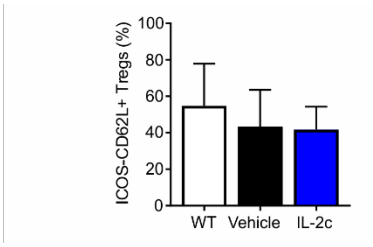

Supplementary Figure 3. Effect of IL-2c treatment on naïve/memory Tregs in SOD1^{G93A} mice. FACS analysis of Treg cell populations in peripheral blood isolated from mice at 100 days of age showing percentage of $CD4^{+}FoxP3^{+}$ Tregs that are $ICOS^{-}CD62L^{+}$ for WT (n = 4), vehicle (n = 5) or IL-2c treated (n = 5) SOD1^{G93A} mice. Data are mean ± SD. Significance was determined using one-way ANOVA with Tukey's multiple comparisons post-hoc test.

Supplementary Figure 4

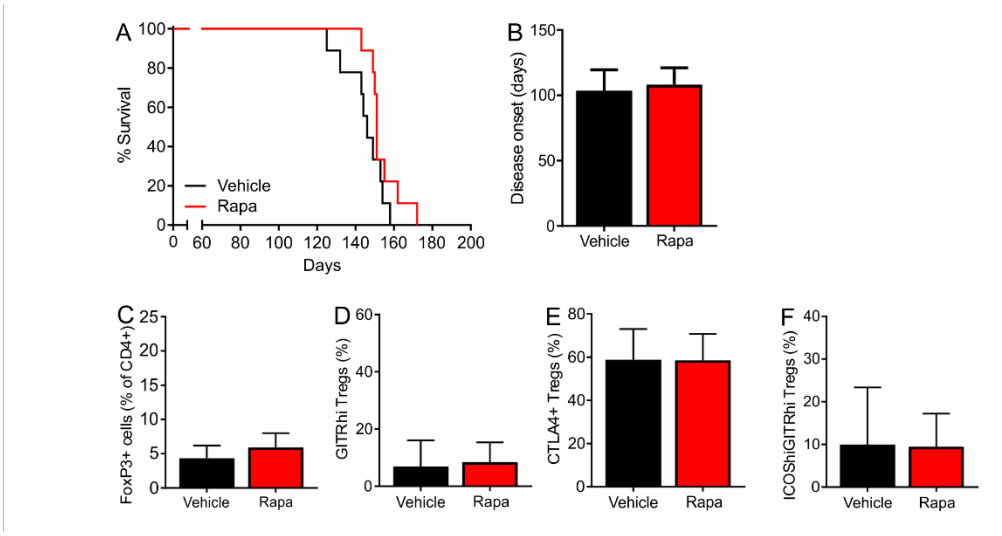

Supplementary Figure 4. Effect of rapamycin treatment on T cell frequencies, disease onset and survival in SOD1^{G93A} mice. **(A)** Survival, defined by hindlimb paralysis, of rapamycin (rapa) treated mice was not significantly different to vehicle group, P>0.05 using Kaplan-Meier survival analysis with the log-rank test. **(B)** Disease onset determined by appearance of body weight loss were not affected by rapa treatment using an unpaired t-test. Data are mean ± SD, n = 9 mice per group. FACS analysis of Treg cell populations in peripheral blood isolated from vehicle and rapa treated SOD1^{G93A} mice at 100 days of age showing percentages of **(C)** CD4^{+} cells that are FoxP3^{+}, and percentage of CD4^{+}FoxP3^{+} Tregs that are **(D)** GITR^{hi}, **(E)** CTLA4^{+}, **(F)** ICOS^{hi}GITR^{hi} for vehicle (n = 5) or rapa treated (n = 5) SOD1^{G93A} mice. Data are mean ± SD. Significance was determined using an unpaired t-test. Note the same vehicle control group was used as shown in Figure 2.

Supplemental Fig 5